Biodegradation of polyester polyurethane by *Aspergillus flavus* G10

Sehroon Khan[1, 2†], Sadia Nadir [†1,2,3], Yang Dong [†4,5] , Douglas A. Schaefer[2*] , Peter E. Mortimer[1], Heng Gui[1,2], Afsar Khan[6], Mingming Yu[7], Shahid Iqbal[1, 2], Jun Sheng[4, 5] Jianchu Xu[1,2*]

[1] Key Laboratory for Plant Biodiversity and Biogeography of East Asia (KLPB), Kunming Institute of Botany, Chinese Academy of Science, Kunming 650201, Yunnan, China.

[2] Centre for Mountain Futures (CMF), Kunming Institute of Botany, Chinese Academy of Science, Kunming 650201, Yunnan, China.

[3] Department of Chemistry, Faculty of Sciences, University of Science and Technology Bannu, Khyber Pakhtunkhwa, 28100 Bannu, Pakistan.

[4] State Key Laboratory for Conservation and Utilization of Bio-Resources in Yunnan, Yunnan Agricultural University, Kunming, 650201, China

[5] Yunnan Research Institute for Local Plateau Agriculture and Industry, Kunming, 650201, China

[6] Department of Chemistry, COMSATS University Islamabad (Abbottabad Campus)-22060, Pakistan.

[7] State Key Lab Phytochemistry & Plant Resources West China, Kunming Institute of Botany, Chinese Academy of Science, Kunming 650201, Yunnan, China.

***Corresponding authors:** Prof. Dr. Jianchu Xu

Email address: jxu@mail.kib.ac.cn

23 Dr. Douglas A. Schaefer

24 Email address: xiedaoan@xtbg.ac.cn

25 † These authors have contributed equally to this work

26 Abstract

27 Polyurethanes (PU) are integral to many aspects of our daily lives. Due to the
28 extensive use of and difficulties in recycling or reusing PU, it mostly accumulates as
29 waste. Various bacteria and fungi have been reported to degrade PU. We examined
30 the fungus *Aspergillus flavus G10* in that regard, after isolating it from the guts of
31 *Gryllus bimaculatus*, a common cricket species. We observed surficial and chemical
32 changes of PU with atomic force microscopy, scanning electron microscopy, and
33 attenuated total reflectance Fourier-transform infrared spectroscopy. We measured
34 physical changes as loss in tensile stress, stretching force, and weight of PU after
35 incubations. Fungal hydrolysis of urethane bonds in the polymer backbone was
36 demonstrated by detecting the formation of methylene di-aniline during incubations.
37 Trapped CO_2 during incubations equaled 52.6% of PU carbon. Biodegradation of PU
38 was maximal by fungi cultured on a malt extract medium at 25 ºC, pH 12, and 14:10
39 hrs light to dark ratio. Pretreating PU films with UV light or 1% $FeSO_4$ or NaCl
40 solutions further enhanced the rate of biodegradation. A range of techniques are
41 needed to fully characterize the degradation of PU or other plastic polymers and to
42 optimize conditions for their microbial degradation.

43 Introduction

44 Annual production of plastics increased to 355 million tones (Mt) in 2017 due to

45 societal and commercial benefits [1]. 9150 Mt of primary plastics have been produced
46 from 1950 to 2015, resulting in 6945 Mt of plastic waste on the surface of earth [2].
47 However, not all plastic waste products are landfilled, incinerated, or recycled.
48 Environmental persistence of plastic waste can produce pollutants that have been
49 shown to be threatening to life in different ecosystems [3, 4, 5, 6].

50 Polyurethane (PU) is a wisely used plastic, accounting for about 7% of total
51 plastic production, with a global annual production of 12 Mt [2]. In China alone the
52 annual production of polyurethane reached 7.5 Mt in 2011 [7]. Incineration and
53 chemical recycling of PU waste are not feasible solutions to PU recycling. In light of
54 this, microbial degradation is one of the most environmentally friendly and
55 cost-effective ways to manage PU waste [7].

56 Many studies examine the microbial degradation of plastics [8, 9, 10] or PU
57 biodegradation alone [11, 12, 13, 14, 15, 7]. Matsumiya et al. [16] reported a 27.5%
58 weight decrease in ether-type PU after 10 weeks' incubation with the fungus
59 *Alternaria sp*.

60 Various methods are used to visualize types and extent of polyurethane
61 biodegradation by fungi or other microbes. According to Khan et al. [11], the holes,
62 pits, and other signs of erosion that were revealed in the scanning electron
63 microscopic (SEM) analysis of the PU films showed biodegradation. Bombelli et al.
64 [17] used Atomic Force Microscopy (AFM) analysis to analyze the surface
65 degradation of *Galleria mellonella* homogenate on the surface of PE. Others used
66 Attenuated Total Reflection Fourier Transform Infrared (ATR-FTIR) spectra to

67 determine chemical alterations in treated and untreated plastics samples [11, 18, 19,
68 20, 21]. Loss of tensile strength also indicates biodegradation [22, 23, 24].

69 Khan et al. [11] used tween 20 and 80 to reduce the hydrophobicity of the PU
70 film surface to make it accessible for fungal spore attachment. Khan et al. [11]
71 demonstrated high enzyme activity at 37ºC in acidic liquid broth culture of *A.*
72 *tubingensis*. Idnurm and Heitman [25] demonstrated that the endophytic fungus was
73 able to sense darkness and use that as a signal to induce virulence, suggesting the
74 possibility that exposure to different light-to-dark ratios could affect biodegradation.

75 Methylene di-aniline (MDA) is known to be the enzymatic biodegraded
76 compound of polyurethanes used as a model compound to analyze the degradation of
77 polyurethanes by enzymes [26]. The fungal strain PURDK2 was found to be able to
78 hydrolyze both urethane and urea bonds in ether-type PU and utilize degraded
79 compounds as a carbon source [16].

80 Next, we isolated the cricket gut fungus *A. flavus* G10 and tested its
81 biodegradation with culture plate and liquid broth methods. Biodegradation of PU was
82 observed using atomic force microscopy, scanning electron microscopy, and
83 attenuated total reflectance Fourier-transform infrared spectroscopy. We also
84 optimized biodegradation by pretreating PU film with UV exposure and incubation in
85 dilute solutions of NaCl, $MgSO_4$, $ZnSO_4$, $FeSO_4$, and $CuSO_4$ salts to determine
86 optimal PU biodegradability. Furthermore, production of CO_2 and MDA were
87 determined. Our results bring novel insights into the field of biodegradation and offer
88 practical significance for environmental remediation.

Materials and methods

We used PU beads, with the chemical formula "poly [4, 4'-methylenebis (phenylisocyanate)-alt-1, 4-butanediol/di (propylene glycol)/polycaprol-actone]," (Aldrich Chemical Company, Inc. USA). The PU beads (1g) were dissolved in tetrahydrofuran (THF) (Sigma-Aldrich) by being shook in a conical flask for 12 hours at 150 rpm at n room temperature. Dissolved PU was poured into glass Petri dishes for solvent evaporation to make PU films. Two types of PU films were prepared by two different drying methods. Dissolved PU air dried at 50% humidity made foamy films, and when dried in a desiccator, PU films formed were transparent [11].

Biodegradation test on solid medium

Solid medium biodegradation was performed for PU films following the method of Khan et al. [11]. Both foamy and transparent types PU films were used for biodegradation analysis. Six MEA plates were prepared according to the manufacturer's instructions. Three MEA plates at pH 7.6, containing transparent PU or foamy PU films, were inoculated with 0.4 ml spore suspension ($1x10^5$ spores/ml) of *A. flavus* G10. Those plates were incubated at 30 ^oC for 28 days. MEA plates containing PU films with no fungal inoculum were used as controls.

Biodegradation in liquid medium

A. flavus G10 was tested for PU biodegradation in a broth culture of malt extract at pH 7.6. Three Erlenmeyer flasks containing 300 ml of malt extract broth were inoculated with 2 ml/flask spore suspension ($1x\ 10^5$ spores/ml) of *A. flavus* G10. Two PU transparent films (90 mm) were cut longitudinally, sterilized with UV radiation

for 5 minutes by exposing the PU films inside laminar flow hood, and were added into each of three Erlenmeyer flasks and incubated at 30 ºC (150 rpm) using a Zhicheng incubator shaker (ZWF 200). After 24, 48, and 72 hours of incubation, samples were collected and brushed gently in sterilized water for one minute. Three PU films immersed in malt extract (ME) broth at pH 7.6, having no fungal inocula, were controls. The liquid biodegradation test was performed for transparent PU films following the method of Khan et al. [11] and repeated for foamy PU films in triplicates. To visualize biodegradation, scanning electron microscopy (SEM) studies were carried out by using the ZEISS Sigma 300 with accelerating voltage from 3 to 7KV; magnification from 50 X to 4500 X; and resolution from 200 µm to 200 nm for both transparent and foamy PU films.

Biodegradation rates of PU film

75 transparent PU films were prepared and exposed to UV for 10 minutes in a laminar flow hood, with 5 minutes on each surface. The initial weight of each film was then measured, and the films were next placed on the *A. flavus* G10 culture in covered Petri dishes. For 15 consecutive weeks, five PU films were removed and washed gently with sterilized water to remove mycelial mass from PU film surfaces. PU films were then dried at room temperature and reweighed. Using the mean values of the 15 weeks, the % DE of the fungus was determined according to the following formula:

$$\% \text{ DE} = \frac{Wt0 - Wtn}{Wt0} \times 100$$

Wt_0 is the initial weight of PU film and Wtn is the weight of PU film after each incubation period (n =1 to 15 weeks). Mean % DE values accumulated over time were

133 treated as efficiency of fungal degradation.

134 Surface topological studies of transparent PU films

135 To assess the effects of *A. flavus* G10 on the surface topology of transparent PU films,
136 mycelia of *A. flavus* G10 were crushed with a mortar and pestle, spread onto three
137 transparent PU films, and then incubated at 37 ºC for two, four, or six hours. PU films
138 were gently brushed with sterilized water and stored at room temperature. Three PU
139 films were established as controls by spreading autoclaved crushed hyphal masses on
140 PU films. Atomic force microscopy (AFM) analysis was used to visualize the surface
141 topology of PU films using AFM (Dimension Icon, Veeco, USA). The AFM was set
142 at 2000 nm and three-dimensional images were scanned.

143 Chemical analysis of the biodegradation of the PU films

144 To explore bond breakage or formation, we performed infrared spectral analysis
145 following the method of Khan et al. [11]. Three replicates of incubated and control
146 transparent PU films were used for analysis. Infrared spectra of these were obtained
147 with an attenuated total reflectance (ATR) accessory for Fourier-transform infrared
148 (FTIR) spectrophotometer (Thermo Scientific Nicolet 10). The spectral range was
149 4000 to 600 cm^{-1} with a resolution of 4 cm^{-1}. Samples were placed on the ATR spot
150 of the additional ATR portion and pressed slowly.

151 Mechanical properties of the PU film exposed to *A. flavus*
152 G10

153 To characterize mechanical properties after biodegradation, transparent PU films
154 (n=11) were exposed to *A. flavus* G10 on a solid medium at 30 ºC for a period of four

155 weeks. After every week, three PU films were randomly selected and brushed with
156 sterilized water and stored at room temperature until analysis. This process was
157 continued until the end of 4th week. A set of three transparent PU films that was not
158 exposed to *A. flavus* G10 were controls.

159 Tensile properties were measured with Biotester 5000 (CellScale, Canada). The
160 amount of force required to stretch PU films (1 cm^2) longitudinally (gage length L_0) to
161 double its original length ($2L_0$) was calculated for both experimental and control PU
162 films. The Biotester 5000 was set at 0.1 mm/s using displacement control with five
163 repetitions for each, at a temperature of 18±2 ºC. Photographs were taken at L_0 and
164 $2L_0$. From the data obtained from Biotester 5000, other mechanical properties such as
165 tensile stress and strain were calculated as below:

166 $$S=\frac{Lmax - L0}{L0} = \frac{\Delta L}{L}$$

167 where S is the strain, and L_{max} is the stretched length of the PU film; and

168 $$\sigma_{max} = \frac{F_{max}}{A_{min}}$$

169 where σ_{max} is the tensile stress, F_{max} is the maximum amount force on the PU film,
170 and A_{min} is the area of the PU film exposed to applied maximum force.

171 An electronic caliper (Chuanlu Measuring Tools, Co. LTD, Shanghai) was used to
172 measure thickness of the PU films. Measurements were made every week for a period
173 of four weeks (Wk1 to Wk4).

174 LC/MS analysis of the PU degraded compounds

175 Haugen et al. [27] used cholesterol esterase for enzymatic degradation of
176 polyurethane to test the biostability of the polymer and found MDA as a

177 biodegradation product. We determined MDA after the biodegradation of PU with *A.*
178 *flavus* G10 following the method of Johnson et al. [28]. The mycelium of *A. flavus*
179 G10 along with the degraded PU film residues (5 g) obtained from the test culture
180 plate were added into conical flasks with 20 ml of a 1:1 methanol and ethyl acetate
181 solution. The mixture was filtered through filter paper and solvent was evaporated. 10
182 mg of obtained solid residue was dissolved in 5 ml acetonitrile, having 0.1% acetic
183 acid to make a suspension. The suspension was centrifuged for 10 minutes at 12000
184 rpm at room temperature. The supernatant was collected and used for liquid
185 chromatography–mass spectrometry (LC-MS) analysis to determine MDA. Another
186 solution was prepared to use as a negative control for LC/MS by adding mycelium
187 and MEA (5 g) obtained from fungal culture plate without PU in the same way as
188 described above. This was used as a negative control. A standard solution of 4,
189 4'-Methylenedianiline (MDA) was prepared by dissolving 0.05 g in 1 mL of
190 acetonitrile with 1% acetic acid. The mixture was centrifuged at 12000 rpm for 10
191 minutes and the supernatant collected for LC-MS analysis. A non-degraded PU film
192 was used as a control.

193 High performance liquid chromatography (HPLC) was performed using the
194 Agilent 1200 Infinity system equipped with a semi-preparative C-18 column (5 µm,
195 250 mm × 4.6 mm). A gradient method was developed to analyze the degradation
196 products [28]. A 10% to 100% solution of a mobile phase consisting of 0.05 M
197 NH_4OAc solution in water (solvent A), as well as HPLC-grade acetonitrile (solvent
198 B), were used to flush the column over a period of 38 minutes at a flow rate 1 ml/min.

The UV absorbance of the eluate was monitored at 254 nm and the fractions corresponding to each HPLC peak were collected. Product identities were confirmed by Electronspray ionization mass spectrometry (ESI-MS) (Agilent G6230), using a direct insertion probe.

Mineralization of PU

The mineralization of PU was determined by measuring the production of CO_2 following the methods of Chinaglia et al. [29]. The conversion of PU carbons to CO_2 by *A. flavus* G10 was assessed for incubation periods of 3, 6, 9, and 12 days. A 2000 mL glass jar containing five MEA Petri dishes inoculated with *A. flavus* G10 (400 µl spore suspension ($1x10^5$ spores/ml) and covered with PU films were placed in an incubator at 30 ºC under 8:16 dark to light ratio for 12 days. All the culture plates were inoculated with *A. flavus* G10 for 10 days before use in this experiment. A 500 ml beaker filled with 300 ml of 1 M KOH (CO_2 trapping solution) was also placed in the jar besides culture plates. The 2000 ml glass jar was sealed. A glass jar containing non-inoculated MEA Petri dishes with a PU film was used as a negative control while a glass jar containing *A. flavus* G10 (concentration of $1x10^5$ spores/ml) cultured on MEA Petri dishes (400 µl spore suspension) was used as a positive control. The incubation time was 3, 6, 9, and 12 days and three replicates were used for each measurement period. The CO_2 produced was measured by titrating KOH solutions with 0.5 M HCl using a potentiometric titrator (Orion Star T900, Thermo Scientific, USA). The conversion of PU to CO_2 was estimated by subtracting the average amount of CO_2 produced in the blank to the amount of CO_2 produced in the

PU-containing jars.

Statistical analysis

The averages and standard errors were computed using Microsoft Excel 2016. To compare differences among treatments, we conducted analysis of variance (ANOVA) in R language and when differences were significant, we performed a pairwise difference analyses with a post-hoc analysis using the TukeyHSD function in the package "agricolae" [30] and also used the plotting function in the "ggplot2" package to plot figures. For ANOVA, we checked whether the models met ANOVA assumptions, and if they did not, we transformed. The only case in which the normal distribution of errors was not met was for media treatments, and we performed logit transformation on those data [31].

Results

A. flavus G10 for PU biodegradation

Aspergillus flavus G10 colonized and grew on transparent and foamy PU films, (Fig 1). Surficial fungal growth on surfaces was easily observed with the naked eye. The discoloration of the PU films, along with the holes and pits in the films, were clear markers of biodegradation. Both kinds of PU films were digested in the center of PU films by the fungus while holes, splits, and discolorations can be seen throughout PU films (Figs 1B and D). Both transparent and foamy control PU films appeared plain and smooth (Figs 1A and C). SEM results further confirmed that biodegradation had taken place (Figs 1A-D). Fungal spores, mycelium, and hyphae could be seen growing on foamy PU films (Fig 1D). Similarly, the SEM results of transparent and

foamy PU films exposed to the fungus showed that the fungus grew across PU film surfaces, with the film broken into pieces. Cracks in transparent PU film, with mycelia inside cracks, are shown in Fig 1 (D).

Biodegradation efficiency of *A. flavus* G10 by percentage

The percentage weight of the PU films exposed to *A. flavus* G10 decreased over time, from week 1 (Wk 1) to week 15 (Wk 15). Average weight loss of the treated PU films was 1.9% per week (S1 Fig). Biodegradation efficiency (% DE) of PU films exposed to *A. flavus* G10 significantly increased from Wk 1 to Wk 15. (S1 Fig, $F1 = 9.368$, $P = 0.003$).

Surface topology and chemical analysis of PU-degraded films

Atomic Force Microscopy (AFM) images showed that while control transparent PU film surfaces remained smooth (Fig 2A), surfaces of transparent PU films exposed to *Aspergillus flavus* G10 were rough, with deep, wide grooves (Fig 2B-D). The average roughness (Ra) recorded for the PU films exposed to the fungus was 2.66, 2.72, and 6.59 nm after 2, 4, and 6 hours of incubation, respectively. Ra values for control PU film surfaces were 1.13 nm. The cross-sectional view of control PU film (S2 A Fig) was smoother than treated PU films (S2 B-D Fig). The differences (Δ) in the length of the highest peak (Z) and the length of lowest point of the groove ΔZ observed for the treated PU films were approximately 14.68, 17.89, and 44.5 nm after 2, 4, and 6 hours of incubation with the fungus as compared to the ΔZ value of 12.31 nm for the control PU. The surface percentage-bearing ratio for the treated PU films was 38.34, 2.42,

and 4.32%, after 2, 4, and 6 hours of incubation respectively, while for control PU films it was 0.13%.

AT-FTIR analysis revealed a notable shift in the spectrum of the foamy PU-treated film (3326.17 cm^{-1}) compared to the control (3327 cm^{-1}) PU film (S3 A and B Figs), which corresponded with the NH bond deformation. Furthermore, another band, corresponding to CH_2 asymmetric stretching at 2933.10 cm^{-1} in the control spectra, was observed to have shifted to 2936.64 cm^{-1} in the spectrum of foamy PU film, indicating cleavage of methylene groups on the polymer backbone (S3 A and B Figs). A small band (2866.81 cm^{-1}) that appeared on the shoulder of the methylene band corresponding to symmetric CH_2 stretching had also shifted to 2867.18 cm^{-1} in the test spectrum of foamy PU film. Similarly, a shift in the position of the band representing C-O…H stretching (S3 A and B Figs) was also observed in the spectra of the treated foamy PU film. A sharp band in the control PU film spectrum at 1066.38 cm^{-1} shifted to 1078.17 cm^{-1}, representing non-bonded C-O groups. Another prominent change was in the sharpness and intensity of the band at 1726.92 cm^{-1} for the urethane carbonyl group, indicating an increase in the concentration of free urethane carbonyl groups in treated foamy PU films. AT-FTIR analysis of the transparent PU film indicated that the broad band representing the N-H bonding was found at 3322.51 cm^{-1}, a shift from the control PU films, which exhibited a band at 3327.93 cm^{-1} in treated PU film (S3 C and D Figs). A second peak in control transparent PU film at 3122 cm^{-1} was found to be decreased in intensity in the treated PU film, indicating NH deformation. The band at 2921.49 cm^{-1},

representing CH_2 asymmetric stretching in the control spectrum, shifted to 2934.91 cm^{-1} (S3 C and D Figs) in treated PU films. Furthermore, a small band representing CH_2 symmetric stretching at 2866.19 cm^{-1} in control PU films shifted to 2866.43 cm^{-1} in PU films. A sharp band at 1726.82 cm^{-1} representing urethane carbonyl groups in control PU films shifted to 1727.09 cm^{-1} in the treated transparent PU films. Finally, a sharp band in control PU film spectrum at 1066.38 cm^{-1} shifted to 1078.17 cm^{-1} in transparent treated PU films, representing non-bonded C-O groups (S3 C and D Figs).

Biodegradation of PU films and its effects on mechanical properties. The stretching force measured on control PU films (0.036 mm thick) was recorded to be 1543.34 mN at Wk0 (S4 A Fig). After one week (Wk1) of incubation with *A. flavus* G10, that decreased to 1403.34 mN. The stretching force decreased further during later incubation, i.e., from Wk2 to Wk4 (S4 Fig), showing significant difference ($p= 0.0015$) (S4 Fig). Prior to incubation, control PU films at Wk0 in normal position (S5 A Fig) and stretched position (S5 B Fig) were completely plain and transparent with no signs of biodegradation. The formation of stains, holes, and deformations increased with time of incubation from Wk2 to Wk4 (S5 Figs). The tensile stress of control PU film was 20.65 Kpa, and that of treatments in Wk1, Wk2, Wk3, and Wk4 were 17.31, 19.01, 16.48, and 10.45 Kpa, respectively, suggesting that tensile strength decreases significantly with exposure to *A. flavus* G10 (S4 B Fig). Differences were highly significant ($p=0.005$) across weeks. The longitudinal strain for the PU film at Wk0 was 0.8713, and those of Wk1, Wk2, Wk3, and Wk4 films were 0.8502, 0.9306, 0.9364, and 0.9614, respectively. There were significant differences among strain

values at different weeks, and the deformation rate increased from W1 to W4 (S4 C Fig) (p=0.007).

PU degradation by *A. flavus* G10 and formation of MDA

LC/MS showed a peak with an m/z value of 199.1237 ([M+H], m/z: calculated as 199.1157 for $C_{13}H_{14}N_2$) that appeared in both the positive control (MDA) and in PU films exposed to *A. flavus* G10 (Figs 3A-a, c and e). This showed that the degradation of PU film was accompanied by the formation of MDA. It did not appear in the negative control or control PU films (Figs 3A - b and f).

Mineralization of PU carbons to CO_2

Conversion of PU to CO_2 increased from 22.3% to 52.6% during the 12-day incubation period (Fig 3B). There were significant differences among CO_2 production across days 3, 6, 9, and 12 (P = 0.01) (Fig 3B).

Discussion

Biodegradation of PU by *Aspergillus flavus* G10

This study is the first to report on the isolation and identification of a PU-degrading fungus from the intestine of crickets. *Aspergillus flavus* G10 can degrade PU efficiently, with a mean weight loss of 1.9% per week. The present study offers practical significance for designing and implementing a sustainable PU waste management strategy as well as insight into the usage of biological agents in large-scale biodegradation platforms. Preliminary screening based on gravimetric analysis (data not shown) identified that the biodegradation of PU by *A. flavus* G10 was significantly higher when grown on solid MEA media as compared to the liquid

331 culture media. Analysis of the surface of the PU exposed to *A. flavus* G10 revealed
332 that PU films had been broken down, were replete with numerous holes and cavities,
333 and that fungal spores and hyphae covered the surfaces of these PU films (Figs 1-3).
334 Similar results, such as the formation of holes in the PU film, hyphal growth on its
335 surface, and discoloration, were previously reported for the biodegradation of PU by
336 *A. tubingensis* [11]. AFM also analysis revealed that the surface of the PU films
337 incubated with *A. flavus* G10 had extensive holes, cavities, and pits. Moreover, cavity
338 depth was observed to increase based on lengthier incubation time (S2 Fig). Similar
339 previous work used AFM to analyze surface degradation of PE [32, 17]. These
340 findings provide clear evidence that *A. flavus* G10 can cause significant damage to the
341 physical integrity of PU films.

342 ATR-FTIR analysis clearly indicated significant shifts in the spectral bands
343 associated with C-H and N-H bonds in the chemical structure of the PU films exposed
344 to *A. flavus* G10. These observations are consistent with past studies that found
345 deformations in the C-H and N-H bonds of PU exposed to *A. tubingensis*, and the
346 observations were attributed to enzymes or radicals released by the fungus [11, 18].
347 Furthermore, our results demonstrated an increase in the intensity and sharpness of
348 bands assigned to free urethane groups, further confirming PU biodegradation by *A.*
349 *flavus* G10 (S3 Fig). Significant losses were observed in the mechanical properties of
350 PU films incubated with *A. flavus* G10, indicating a decline in physical integrity of the
351 films as a result of its growth and enzymatic activities (S4 and S5 Figs). Similar
352 results for the loss of tensile strength in PU films due to biodegradation have been

353 previously reported [11, 22, 23, 24, 33]. Yang et al. [32] reported approximately 50%
354 loss in tensile strength due to bacterial biodegradation of polyethylene film. In
355 addition to a breakdown of the mechanical properties of the PU films, those films
356 exposed to *A. flavus* G10 exhibited a steady rate of mass loss over the course of 15
357 weeks. Past studies have shown similar trends in PE films exposed to bacteria capable
358 of digestion [32, 33, 34], but PU mass loss was higher in this case.

359 ## Optimizing the efficiency of biodegradation

360 Of the different media we tested, *A. flavus* G10 performed best on MEA, with high
361 biodegradative capabilities. The growth rate of *A. flavus* G10 was three times higher
362 when grown on MEA in comparison with other media used in our study (S6 Fig).
363 However, this preference for MEA by *A. flavus* G10 appears to be quite specific, as it
364 has been shown that *A. tubingensis*, another fungus capable of degrading PU, grew
365 best on MSM media compared to PDA and SDA when isolated from soil [11]. Thus,
366 any trials investigating fungal growth and biodegradative capacity should first test for
367 which media is optimal.

368 We also showed that temperature, pH, and photoperiod were important factors
369 that influence the performance and biodegradative capacity of *A. flavus* G10. The
370 optimum temperature for *A. flavus* G10 was found to be 25ºC, and as temperature
371 increased, the rate of biodegradation began to decline, before becoming totally
372 inhibited at 40ºC (S6 D Fig). Khan et al. [11] previously demonstrated high enzyme
373 activities at 37ºC in the liquid broth culture of *A. tubingensis*. The difference in the
374 temperature optimum of these fungi may reflect genetic differences. It appears that

375 the ideal pH range for fungal growth is related to the environment from which the
376 fungus was isolated. *Aspergillus flavus* G10 was isolated from an alkaline
377 environment in the gut of a cricket, and was found to perform best in alkaline media,
378 with an optimal pH of 12 (S7 Fig). Confirming our assumption that optimal pH for
379 fungal growth is closely related to the environment from which it originates, the most
380 ideal pH for degradation of PU by *A. tubingensis* was slightly acidic, as it was
381 originally isolated from acidic soil conditions [11]. Numerous photoperiods were
382 tested here and it was determined that light to dark ratios of 8:16 and 14:10 are
383 optimal for the growth and biodegradative abilities of *A. flavus* G10 (S6 Fig).

384 In addition to optimizing the environmental conditions for *A. flavus* G10, adding
385 salts to the growing media (MEA) was found to have significant effects on the
386 biodegradation process. $MgSO_4$ was found to accelerate biodegradation (S7 Fig). Not
387 all salts improved the performance of *A. flavus* G10: $CuSO_4$ and $ZnSO_4$ were found to
388 inhibit fungal activity. No past studies have investigated the effects of adding salts to
389 fungi degradation, so this research suggests possibilities for future work.

390 We have shown that the manipulation of media and environmental conditions can
391 significantly influence the biodegradative capacity of *A. flavus* G10; however, we also
392 found that treating the PU films before incubation with *A. flavus* G10 also changed
393 rates and extent of fungal degradation. Past studies have shown that photo, thermal, or
394 chemical treatments of polymers prior to microbial exposure can increase
395 biodegradation [7, 35]. In this study, we performed photo- and chemical-based
396 pre-treatments. We observed that PU films exposed to solutions of either $FeSO_4$,

$7H_2O$, or NaCl prior to *A. flavus* G10 incubation experienced increased rates biodegradation efficiencies (S7 Fig). Exposure of PU films to certain salts decreases the hydrophobicity of the PU films, thereby enhancing the biodegradation of polymers [7]. Shangguan et al. [36] evaluated the effects of UV on the bacterial biodegradability of bio-polyester poly (3-hydroxybutyrate-co-3-hydroxyhexanoate) and found high rates of biodegradation by exposing polyester powder or film to UV radiation. Consistent with previous research [36], we also found that PU films exposed to UV radiation for 5 min prior to incubation with the fungus showed increased biodegradation (S6 Fig). It has been reported that UV radiation results in surface changes in polymers that microorganisms can access more easily [37]. However, according to this study, a longer exposure time to UV radiation led to a decline in the rates of biodegradation. This may relate to the lower or negligible degradation of PU in landfill and dumping sites.

Biodegradation of PU by *A. flavus* G10 and production of MDA

Methylene di-aniline (MDA) is known to be the enzymatic biodegradation product of PU [27]. Our results detected high concentrations of MDA in the degradation medium, indicating that *A. flavus* G10 was successful in breaking down PU by secreting hydrolytic enzyme(s). Based on these findings, we suggest that PU biodegradation by *A. flavus* G10 occurs in a two-phase process. In the first phase, the fungus colonizes the surface of the PU and causes physical disruption of PU via hyphal growth. Next, the fungus secretes hydrolyzing enzyme(s) that depolymerize

PU into low–molecular-weight compounds. These compounds are utilized by the fungus for its own energy and converted into CO_2 and H_2O. In a previous study, the fungal strain PURDK2 was found to be able to hydrolyze both the urethane and urea bonds in the ether-type PU, and utilize the degraded compounds as a carbon source [16]. Our results suggest that production of aromatic amines such as methylene di-aniline (MDA) from PU biodegradation (S3 A Fig) could lead to the chemical recycling of PU; however, further experiments are needed in this area.

Mineralization of PU

The incubation of PU with *A. flavus* G10 resulted in the production of CO_2, and after 12 days of incubation, the amount of released CO_2 was the equivalent of about 52.6% of the C in the PU film (Fig 3). Zumstein et al. [38] have identified that the carbon derived from the biodegradation of poly (butylene adipate-co-terephthalate) polymer is converted into CO_2 and microbial biomass [38]. They observed the ^{13}C-labeled isotopic carbon to develop the synthetic polymer, and the isotopic carbon was seen both in the fungal mycelia and in the evaluated CO_2. Future studies that build upon on our work using ^{13}C-labeled polymer would help us trace the exact fate of PU-derived carbons as well as monitor to what extent the fungus is able to assimilate the C for growth.

Acknowledgments

This work was supported by the Chinese Academy of Sciences, President's International Fellowship Initiative (CAS-PIFI), and Key Research Program of Frontier Sciences, CAS. We are thankful to Zhijia Gu, Key Laboratories for Plant

Diversity and Biogeography of East China, Kunming Institute of Botany, Chinese Academy of Sciences, for his high level of support in using the scanning electron microscopy for photography.

References

1. Plastics Europe. Plastics the Facts. 2017. Available online: http://www.plasticseurope.org/en/resources/publications/plastics-facts-20173 (accessed on 15 March 2018).

2. Geyer R, Jambeck JR, Law KL. Production, use, and fate of all plastics ever made. Sci Adv. 2017; 3: e1700782.

3. Rillig MC, Bonkowski M. Microplastic and soil protists: a call for research. Environ Pollut. 2018; 241: 1128-1131.

4. Worm B, Lotze HK, Jubinville I, Wilcox C, Jambeck J. Plastic as a persistent marine pollutant. Annu Rev Environ Resour. 2017; 42: 1–26.

5. Barnes DKA, Galgani F, Thompson RC, Barlaz M. Accumulation and fragmentation of plastic debris in global environments. Philos Trans R Soc Lond B: Biol Sci. 2009; 364: 1985–1998.

6. Thompson RC, Moore CJ, Von Saal FS, Swan SH. Plastics, the environment and human health: Current consensus and future trends. Philos Trans Royal Soc. 2009; 364: 2153–2166.

7. Cregut M, Bedas M, Durand MJ, Thouand G. New insights into polyurethane biodegradation and realistic prospects for the development of a sustainable waste recycling process. Biotechnol Adv. 2013; 31: 1634–1647.

463 8. Ojeda TFM, Dalmolin E, Forte MMC, Jacques RJS, Bento FM, Camargo FAO.
464 Abiotic and biotic degradation of oxo-biodegradable polyethylenes. Polym Degrad
465 Stabil. 2009; 94: 965-970.
466 9. Jeyakumar D, Chirsteen J. Doble M. Synergistic effects of pretreatment and
467 blending on fungi mediated biodegradation of polypropylenes. Bioresour Technol.
468 2013; 148:78-85.
469 10. Restrepo-Flórez JM, Bassi A, Thompson MR. Microbial degradation and
470 deterioration of polyethylene–A review. Int Biodeterior Biodegrad. 2014; 1: 88:83-90.
471 11. Khan S, Nadir S, Shah ZU, Shah AA, Karunarathna S, Xu J, et al. Biodegradation
472 of Polyester Polyurethane by Aspergillus Tubingensis. Environ Pollu. 2017; 225:
473 469-480 https://doi.org/10.1016/j.envpol.2017.03.012.
474 12. Howard GT, Norton WN, Burks T. Growth of Acinetobacter gerneri P7 on
475 polyurethane and the purification and characterization of a polyurethanase enzyme.
476 Biodegradation. 2012; 23:561–567.
477 13. Zafar U, Houlden A. Robson GD. Fungal communities associated with the
478 biodegradation of polyester polyurethane buried under compost at different
479 temperatures. Appl. Environ. Microbiol. 2013; 79: 7313-7324.
480 14. Zafar U, Nzeram P, Langarica-Fuentes A, Houlden A, Heyworth A, Saiani A, et
481 al. Biodegradation of polyester polyurethane during commercial composting and
482 analysis of associated fungal communities. Bioresour Technol. 2014; 158: 374-377.
483 15. Mathur G, Prasad R. Degradation of polyurethane by Aspergillus flavus (ITCC
484 6051) isolated from soil. Appl Biochem Biotechnol. 2012; 167: 1595-1602.

485 16. Matsumiya Y, Murata N, Tanabe E, Kubota K, Kubo M. Isolation and
486 characterization of an ether-type polyurethane-degrading micro-organism and analysis
487 of degradation mechanism by Alternaria sp. J Appl Microbiol. 2010; 108: 1946–1953.

488 17. Bombelli P, Howe CJ, Bertocchini F. Polyethylene bio-degradation by caterpillars
489 of the wax moth *Galleria mellonella*. Curr Biol. 2017; 27: R292-R293.

490 18. Bressan F, Bertani R, Furlan C, Simionato F, Canazza S. An ATR-FTIR and
491 ESEM study on magnetic tapes for the assessment of the degradation of historical
492 audio recordings. J Cult Herit. 2016; 18: 313-320.

493 19. Gonon L, Mallegol J, Commereuc S, Verney V. Step-scan FTIR and
494 photoacoustic detection to assess depth profile of photooxidized polymer. Vib.
495 Spectrosc. 2001; 26: 43.

496 20. Bokria JG, Schlick S. Spatial effects in the photo degradation of poly (acrylo
497 nitrile-butadiene-styrene): a study ATR-FTIR. Polymer. 2002; 43: 32-39.

498 21. Mailhot BS, Morlat-Therias, Bussiere PO, Gardette JL. Study of the degradation
499 of an epoxy/amine resin, 2 kinetics and depth-profiles. Macromol Chem Phys. 2005;
500 206: 85.

501 22. Tsuji H, Suzuyoshi K. Environmental degradation of biodegradable polyesters 1.
502 Poly (ε-caprolactone), poly [(R)-3-hydroxybutyrate], and poly (L-lactide) films in
503 controlled static seawater. Polymer Degrad Stab. 2002; 75: 347-355.

504 23. Lee SR, Park HM, Lim H, Kang T, Li X, Cho WJ, et al. Microstructure, tensile
505 properties, and biodegradability of aliphatic polyester/clay nanocomposites. Polymer.

506 2002; 43: 2495-2500.

507 24. Ochi S. Mechanical properties of kenaf fibers and kenaf/PLA composites. Mech
508 Mater. 2008; 40: 446-452.

509 25. Idnurm A, Heitman J. Light controls growth and development via a conserved
510 pathway in the fungal kingdom. PLoS Biol. 2005; 3: e95.

511 26. Johnson JR, Daniel K, Marianne D, Gunnar S. Determination of aromatic amines
512 in aqueous extracts of polyurethane foam using hydrophilic interaction liquid
513 chromatography and mass spectrometry Analytica Chimica Acta. 2010; 678:
514 117–123.

515 27. Haugen H, Gerhardt LC, Will J, Wintermantel E. Biostability of
516 Polyether–Urethane Scaffolds: A Comparison of Two Novel Processing Methods and
517 the Effect of Higher Gamma-Irradiation Dose. Appl Biomater. 2005; 73: 229–237.

518 28. Johnson JR, Daniel K, Marianne D, Gunnar S. Determination of aromatic amines
519 in aqueous extracts of polyurethane foam using hydrophilic interaction liquid
520 chromatography and mass spectrometry. Analytica Chimica Acta. 2010; 678:
521 117–123.

522 29. Chinaglia S, Tosin M, Innocenti FD. Biodegradation rate of biodegradable
523 plastics at molecular level. Polym Degrad Stabil. 2018; 147: 237-244.
524 https://doi.org/10.1016/j.polymdegradstab.2017.12.011.

525 30. de Mendiburu F, de Mendiburu MF. Package agricolae. Statistical procedures for
526 agricultural research. 2017.

527 31. Warton DI, Hui FKC. The arcsine is asinine: the analysis of proportions in
528 ecology. Ecology. 2011; 92: 3–10.
529 32. Yang J, Yang Y, Wu WM, Zhao J, Jiang L. Evidence of polyethylene
530 biodegradation by bacterial strains from the guts of plastic-eating wax worms.
531 Environ Sci Technol. 2014; 48: 13776-13784.
532 33. Gilan I, Hadar Y, Sivan A. Colonization, biofilm formation and biodegradation of
533 polyethylene by a strain of *Rhodococcus ruber*. Appl Microbiol Biotechnol. 2004; 65:
534 97-104.
535 34. Sudhakar M, Doble M, Murthy PS, Venkatesan R. Marine microbe-mediated
536 biodegradation of low-and high-density polyethylenes. Int Biodeterior Biodegrad.
537 2008; 61: 203-213.
538 35. Mahalakshmi V, Andrew NS. Assessment of physicochemically treated plastic by
539 fungi. Ann Biol Res. 2012; 3: 4374-4381.
540 36. Shangguan YY, Wang YW, Wu Q, Chen GQ. The mechanical properties and in
541 vitro biodegradation and biocompatibility of UV-treated poly
542 (3-hydroxybutyrate-co-3-hydroxyhexanoate). Biomaterials. 2006; 27: 2349-2357.
543 37. Lu T, Solis-Ramos E, Yi Y, Kumosa M. UV degradation model for polymers and
544 polymer matrix composites. Polym Degrad Stabil. 2018; 154: 203-210.
545 38. Zumstein MT, Schintlmeister A, Nelson TF, Baumgartner R. et al.
546 Biodegradation of synthetic polymers in soils: Tracking carbon into CO_2 and
547 microbial biomass. Sci Adv. 2018; 4: eaas9024.

548

1

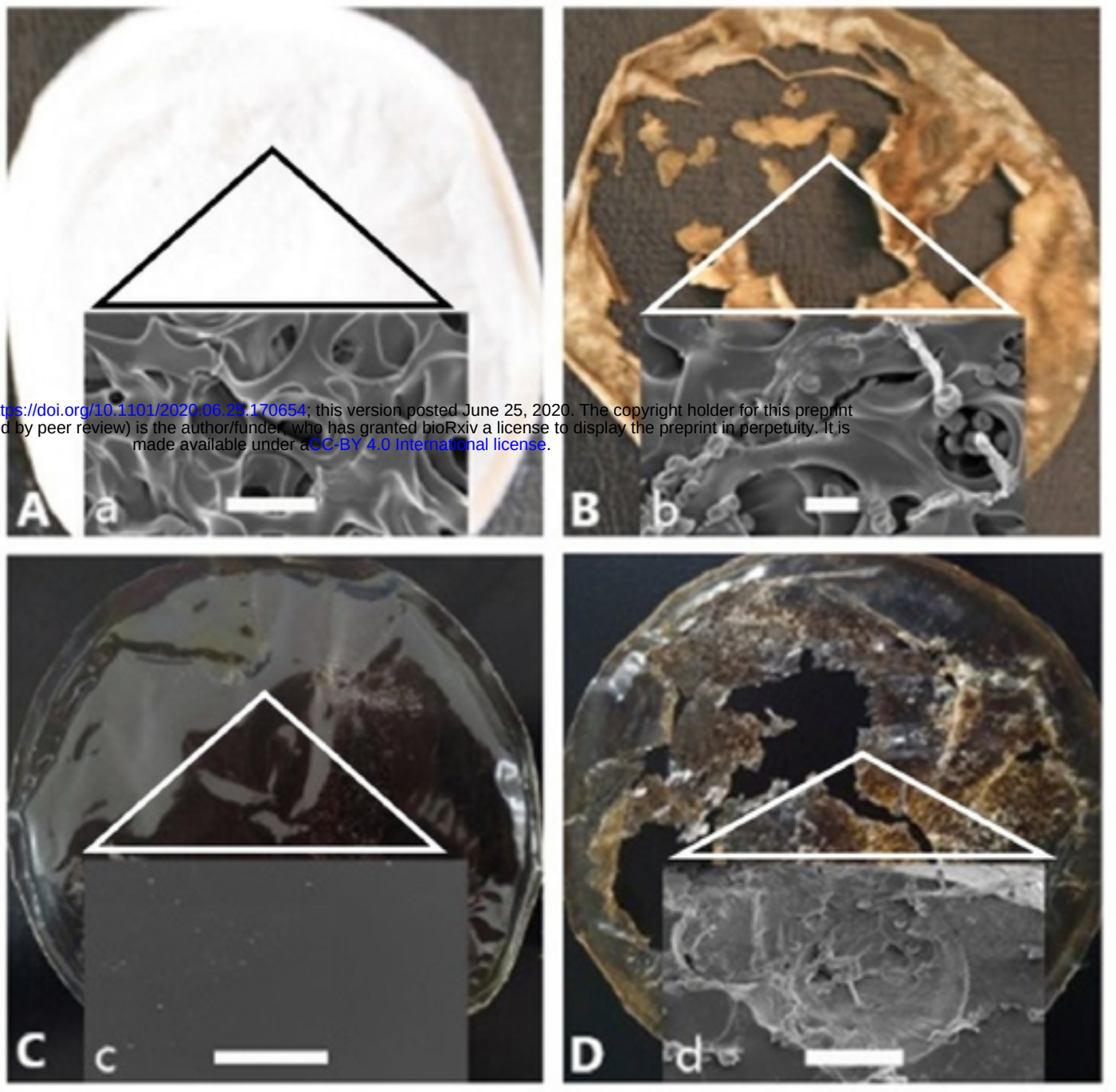

2

3 Fig 1. PU biodegradation by *A. flavus G10*. (a) and (c) represent foamy and

4 transparent control PU films respectively that were not exposed to *A. flavus* G10. (b)

5 and (b) represent foamy and transparent PU films, respectively, that were exposed to

6 *A. flavus* G10 for 28 days. The light green/brown color was the growth of fungus on

7 surfaces of PU films. SEM images of foamy PU films. (a) Control foamy PU. (b)

8 foamy PU exposed to *A. flavus* G10. Fungal spores, mycelia and hyphae can be seen

9 in the SEM image. (c) Control transparent PU film (d) treated transparent PU films.

10 Scale bars a = 10 μm, b = 4 μm, c = 60 μm, and d= 20 μm.

11

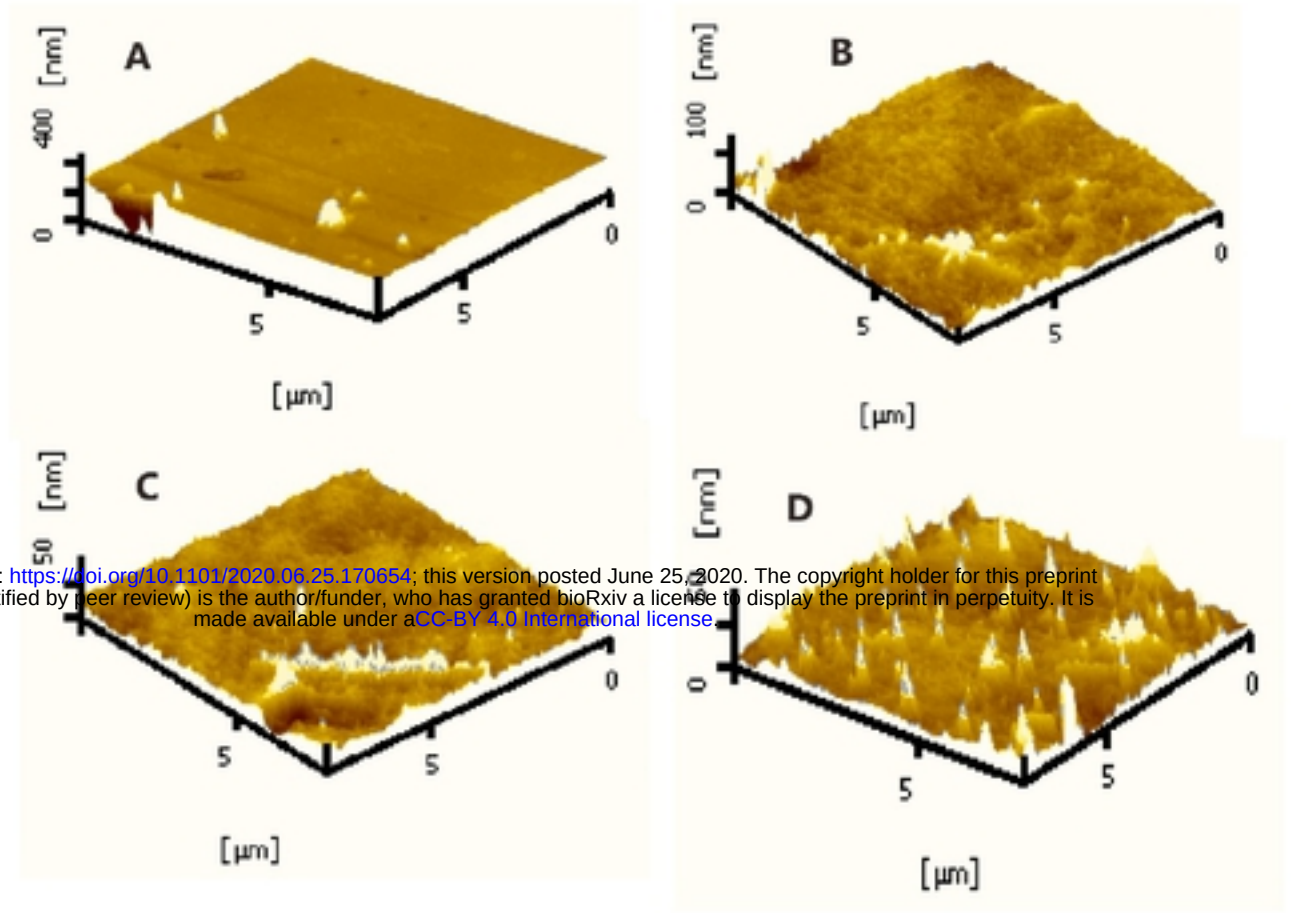

13

14 Fig 2. Three-dimensional (3D) topography of the surface of PU films using AFM. (a)

15 3D surface scan of control PU film. (b-d) 3D surfaces of PU films treated for 2, 4, and

16 6 hours with mashed *A. flavus*. Scan size is 8nm.

17

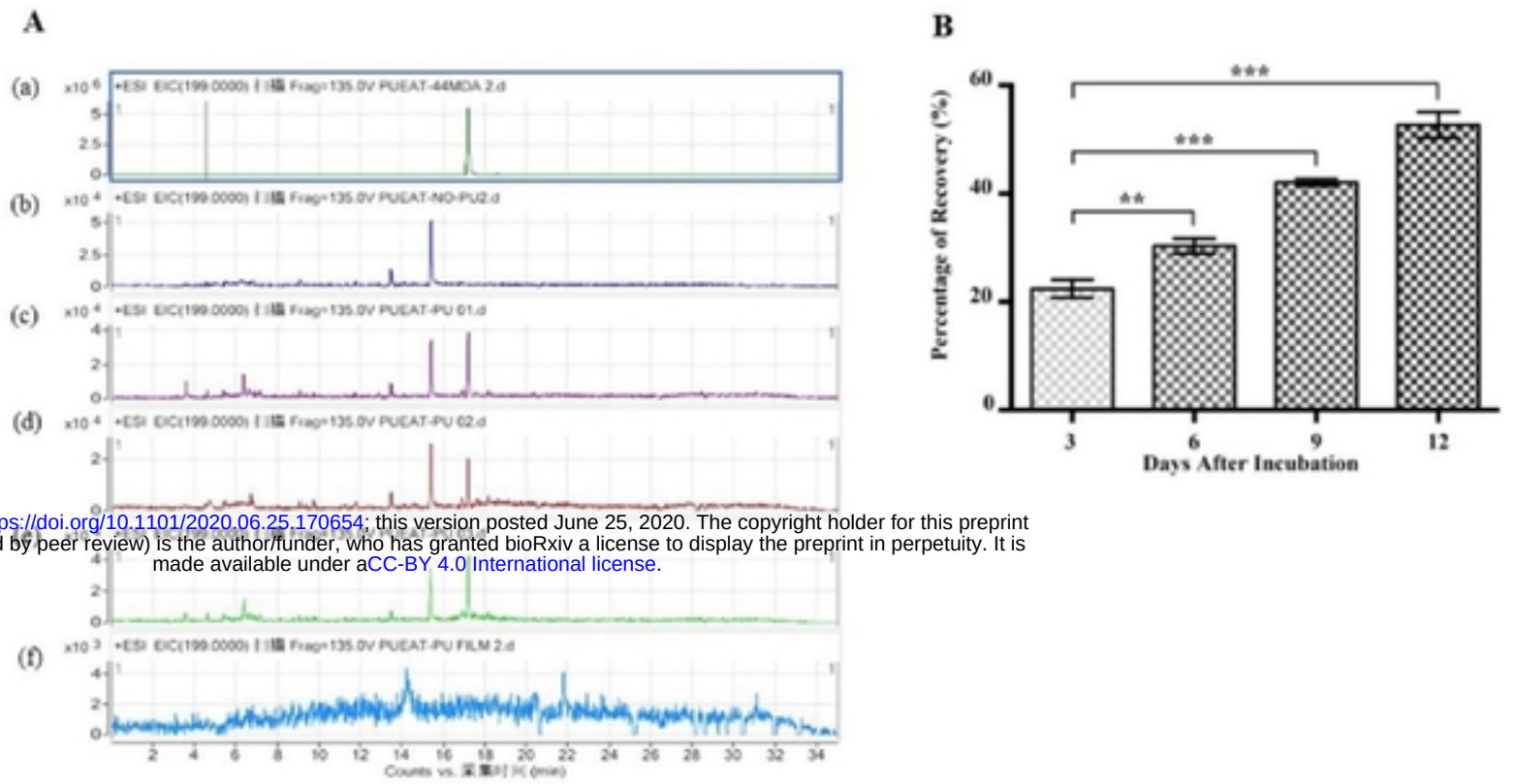

19

20 Fig 3. Urethane bond hydrolysis and mineralization of PU films. (A): LC/MS analysis
21 of urethane bond hydrolysis. (a) MDA as a standard compound. (b) MEA medium
22 and fungal mycelium were used as a negative control. (c, d and e) The peaks of the
23 degraded PU films. (f) Represents a non-degraded PU film. (B) Formation of CO_2
24 from the PU sheets during their incubation with *A. flavus* G10 in glass jars, for 3, 6, 9
25 and 12 days. Results from replicate experiments are shown. The data was analyzed
26 using PRISIM 6.0 for significant difference by the One-way-ANOVA (*P<0.05,
27 **P<0.01, ***P<0.001).

28

29